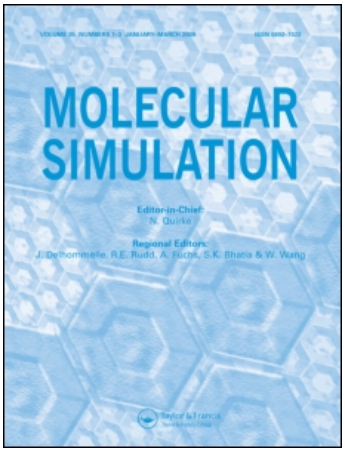

Molecular Simulation

Publication details, including instructions for authors and subscription information:
http://www.informaworld.com/smpp/title~content=t713644482

Nanoscale van der Waals interactions

Milton W. Cole[ab]; Darrell Velegol[bc]; Hye-Young Kim[d]; Amand A. Lucas[e]
[a] Department of Physics, The Pennsylvania State University, University Park, PA, USA [b] Materials Research Institute, The Pennsylvania State University, University Park, PA, USA [c] Department of Chemical Engineering, The Pennsylvania State University, University Park, PA, USA [d] Department of Chemistry and Physics, Southeastern Louisiana University, Hammond, LA, USA [e] Laboratoire de physique du solide, Facultes Universitaires Notre-Dame de la Paix, Namur, Belgium

To cite this Article Cole, Milton W. , Velegol, Darrell , Kim, Hye-Young and Lucas, Amand A.(2009) 'Nanoscale van der Waals interactions', Molecular Simulation, 35: 10, 849 — 866
To link to this Article: DOI: 10.1080/08927020902929794
URL: http://dx.doi.org/10.1080/08927020902929794

Molecular Simulation
Vol. 35, Nos. 10–11, September 2009, 849–866

Taylor & Francis
Taylor & Francis Group

Nanoscale van der Waals interactions

Milton W. Cole[ac1], Darrell Velegol[bc]*, Hye-Young Kim[e] and Amand A. Lucas[d]

[a]*Department of Physics, The Pennsylvania State University, University Park, PA 16802, USA;* [b]*Department of Chemical Engineering, The Pennsylvania State University, University Park, PA 16802, USA;* [c]*Materials Research Institute, The Pennsylvania State University, University Park, PA 16802, USA;* [d]*Laboratoire de physique du solide, Facultes Universitaires Notre-Dame de la Paix, 61 rue de Bruxelles, B5000 Namur, Belgium;* [e]*Department of Chemistry and Physics, Southeastern Louisiana University, Hammond, LA 70402, USA*

(*Received 15 December 2008; final version received 24 March 2009*)

Despite the fact that van der Waals (VDW) interactions are often considered to be weak, they dominate the behaviour of all neutral physical systems at separations of order 0.5 nm or larger. For simple geometries – geometric half spaces, spheres, cylinders, or points – VDW interactions are often calculated using a form of Lifshitz theory, which is based on continuum descriptions. But for nanoscale systems, it is often the case that the geometries involve corners, sharp edges, discrete atom placement or small sizes, so that bulk continuum models do not apply. In these cases it is common to compute the VDW interactions using two-body calculations, for instance from Lennard-Jones parameters, the Derjaguin or Hamaker approximation, or pairwise additivity. In this review, we show that none of these estimates predicts VDW interactions accurately; rather, one must use a 'nanoscale Lifshitz theory', which we call the 'coupled dipole method' (CDM). The CDM accounts for all many-body interactions in the nonretarded limit. The method uses an exact evaluation of the eigenmodes of the coupled dipole oscillators, which represent the charge fluctuations of the system. A key quantity determining the relative importance of many-body contributions is the dimensionless ratio ($\nu = \alpha/a^3$) of the polarisability to the cube of the interparticle spacing. We assess the accuracy of two-body and three-body calculations against many-body predictions, and then briefly discuss the role of retardation. Several important research questions remain, and these are summarised.

Keywords: van der Waals interactions; coupled dipole method; nanoscale

1. Introduction

Van der Waals (VDW) interactions are variously described as 'weak' interactions, 'physical' interactions, 'dispersion' interactions or 'non-bonding' interactions between atoms, molecules, clusters, or even larger material bodies. There are in fact two related, but distinct, meanings of the term *VDW interactions*. One is associated with the various kinds of bonding between atoms. Whereas NaCl involves an ionic bond and H_2 has a covalent bond, He–He involves the weak VDW bond [1].[2] The other meaning refers to the fact that at large separations, *any* pair or group of atoms in their electronic ground state experiences a weak attraction associated with charge fluctuations. This latter, more general, meaning of VDW interactions is the subject of the present paper.

VDW interactions are a purely quantum mechanical effect, caused by fluctuations in electronic charge densities throughout the materials. In the ground state these are the zero-point fluctuations, and in thermally excited states these are thermal fluctuations. Despite the fact that VDW interaction energies are often considered to be small, they are important because in many physical systems, they are the *only* attractive interaction of significant magnitude. For instance, it is the presence of a VDW attraction between hexane molecules that enables them to condense into a liquid phase at standard conditions. Similarly, the attraction between two colloidal particles is due, in large part, to VDW forces. At the macroscopic level, the adhesion of two atomically flat surfaces is caused by VDW forces. The cohesion of molecular crystals is insured by VDW forces. In nanoscale systems more generally, VDW forces are responsible for surface tension, solvophobicity/philicity, and nanoparticle aggregation – phenomena that often control nanoscale systems. In biological multimeric proteins, VDW forces contribute to the stability of the system. How does one predict VDW forces for nanoscale systems?

VDW interactions were first hypothesised in the late nineteenth century by J.D. van der Waals in his Ph.D. thesis to explain vapour–liquid equations of state. But not until the advent of quantum mechanics were the origins of VDW interactions explained qualitatively, and even quantitatively, by Fritz London [2]. Many others have since studied these interactions, improving the accuracy of VDW force calculations between atomic or small molecule systems [3,4]. Extending the calculations to large systems has proved challenging, unless one makes the explicit assumption that interactions are pairwise additive; unfortunately,

*Corresponding author. Email: velegol@psu.edu

ISSN 0892-7022 print/ISSN 1029-0435 online

DOI: 10.1080/08927020902929794
http://www.informaworld.com

this is a bad approximation except for materials with low polarisability. A significant advance beyond that approximation was made by Dzyaloshinskii, Lifhsitz and Pitaevskii (DLP) [5], who evaluated VDW interactions exactly, for the case of uniform, continuum media and several simple geometries [6]. In principle, continuum Lifshitz theory (as we call the DLP method) gives the full many-body, retarded interaction for all sizes and all separations between ideal geometries such as spheres [7]. In practice, surface roughness renders the continuum model inadequate at close separations, precisely where the VDW attraction exceeds the thermal energy (kT) for nanoscale systems. Nevertheless, since about 1960 [2,3,4,8], many researchers have considered the prediction of VDW forces, to be straightforward in principle, for *all* situations, especially by Lifshitz theory.

However, at the *nanoscale* VDW forces are not so readily predicted, or even estimated. The nanoscale problem includes these complicating issues: (1) Atoms are located at specific locations, not well characterised by continuum models or simple geometries; their placement includes corners, sharp edges, and roughness that can be comparable to the particle size. (2) Nanoscale systems have a permittivity – a macroscopic concept from electrodynamics – that varies near the boundaries of an object, because of local field effects and/or structural effects, so that the bulk approximation is not adequate. (3) Nanoscale systems sometimes have part of their interacting material sufficiently close for a 'nonretarded' VDW model to be applicable, while other pieces are farther apart, requiring a 'retarded' theory. This distinction will be explained later.

Thus, while Lifshitz theory works well for simple geometries and large regions of the size-separation domain, its continuum aspects limit its utility in regimes that matter most. As a result, one commonly-used approach to computing nanoscale VDW forces is to sum all two-body interactions, thus assuming that each atom interacts with every other atom without other atoms' affecting the interaction between the first two. This approach neglects all *many-body interactions*, i.e. *screening*. A variant of this approach involves the use of a *Hamaker constant* (A) to characterise the VDW interactions between atoms, within the two-body approximation [9]. The original London theory [10] of VDW interactions showed that the interaction energy $V = -C_6/r^6$, where r is the distance between the two atoms and C_6 is evaluated from quantum calculations, using a formula discussed later. In the Hamaker approach, the coefficient C_6 of the VDW interaction is usually evaluated from a solution of the full many-body Lifshitz theory for some *given geometry* – often the interaction between two half-spaces – and then this coefficient is employed in *other geometries*. A fundamental difficulty with this method is that one is applying to one geometry information concerning many-body effects derived from a different geometry. Hence, the C_6 coefficient will *not* be correct, in general, because of the highly nonlinear nature of the VDW interaction. Thus, this approach suffers from all three difficulties enumerated in the preceding paragraph.

Another method that partially uses the pairwise approach is the Derjaguin technique [11]. Here, one mathematically slices a material, calculates the many-body VDW interactions between the slices – and at this point, the method looks like a full many-body calculation – but then simply adds the contributions from the various slices. This last step involves a pairwise sum approach. The Derjaguin approximation is commonly used for fairly symmetric shapes like spheres and spheroids; however, at the nanoscale the method has two limitations that are the same as those of Lifshitz theory. Explicitly, this method assumes geometric objects like spheres or spheroids, as well as a continuum approach.

In most of our calculations of nanoscale VDW interactions, we have used a very different approach. In the limit of small separations where retardation can be ignored, and in the limit of zero temperature, we combine quantum physics, classical electrostatics and classical mechanics to find the VDW energies precisely. This 'coupled dipole method' (CDM) is uniquely positioned to evaluate VDW energies between atoms, molecules, clusters and particles at the nanoscale. Regimes involving particles nearly touching, or with surface roughness, are where the CDM works well, and unlike Lifshitz theory, the CDM is not limited to ideal shapes like spheres, cylinders or half spaces. The method has no difficulty handling *arbitrary* shapes.

Our group has focussed on the many-body contributions to the VDW interaction energy for clusters of varying size and shape. By the term 'many-body', we refer to all corrections to two-body (pair) interactions. Our definition of the many-body correction to the energy, V_{MB}, is this

$$V_{\mathrm{MB}}\{\mathbf{r}_j\} \equiv V\{\mathbf{r}_j\} - V_{\mathrm{T2}}. \tag{1}$$

Here, $V\{\mathbf{r}_j\}$ represents the total VDW energy of the system while V_{T2}, the total two-body energy, is a sum of all pair interaction energies:

$$V_{\mathrm{T2}} = \Sigma_{j<k} V_2(r_{jk}). \tag{2}$$

The distance $r_{jk} = |\mathbf{r}_j - \mathbf{r}_k|$ is the separation between particles j and k and $V_2(r_{jk})$ is the corresponding pair interaction.

There are many open research questions concerning VDW interactions. These questions address the effects of 'retardation', due to the finite speed of light, the collection and assessment of dielectric data for predictions of VDW interactions, the role of finite temperatures and even deeply fundamental issues associated with the Casimir

effect [12]. In this review, we focus on these two important questions: (1) How accurately do two-body interactions represent the full many-body VDW interaction? One finds that two-body models – for example, the Lennard-Jones (LJ) interactions, the 'Hamaker constants' for colloidal particles, and even the Derjaguin approximation [11] that uses some many-body effects – are seldom accurate enough for nanoscale systems. (2) If the two-body prediction is insufficient, how can one more accurately predict the VDW interactions? We aim to demonstrate that for nanoscale systems – neither atomic nor macroscopic/continuum in nature – that the CDM is a practical technique capable of providing accurate predictions of these interactions.

The outline of this paper is the following. The next section provides an overview of the nature of VDW interactions, with some focus on the particular problem of the interaction between a single molecule and a surface. Section 3 describes the CDM, which is a convenient method to determine VDW interactions exactly, in cases where retardation can be neglected. Section 4 summarises the nature of retardation, which is more important than one might expect for nanoscale interactions. Section 5 discusses outstanding problems of particular interest. A series of appendices discuss the justification for the CDM method, the accuracy of the Drude approximation, the many-body expansion of the energy and molecular polarisabilities.

2. Origins of VDW interactions and many-body effects

In this section, we begin with one conceptually simple and mathematically straightforward problem in order to demonstrate the physical origin of VDW interactions and elucidate when and why many-body contributions are important. The problem we consider is the interaction between one atom and a surface of a material which occupies the half-space, $z < 0$. Suppose that the atom and the bounding plane are separated by distance $z \geq 1\,\text{nm}$ (Figure 1); however, z should not be so large that retardation, explained later as resulting from the finite speed of light, significantly influences the interaction. The 'atom' could also be a molecule or small particle if its size is much smaller than the separation z. The interaction is due purely to VDW considerations, since the bonding interactions depend on charge overlap, which decays exponentially with distance from the constituent particles. The asymptotic form of this gas-surface VDW interaction, $V_{\text{gs}}(z)$, is known from DLP theory to satisfy the asymptotic power-law relation:

$$V_{\text{gs}}(z) \sim -C_3/z^3. \tag{3}$$

The exponent '3' appearing in this equation is typically explained in one of two quite different ways. Probably the more common, but less accurate, explanation is that an inverse-cube interaction arises when the potential energy $V_{\text{gs}}(z)$ is derived from a sum (or integral) of two-body VDW interactions, each of which varies as $V_2(r) \sim -C_6/r^6$, over the solid half-space $z' < 0$. If n_{s} equals the number density of its constituent atoms, the result of summing these two-body interactions is equivalent at large z to an integration over the solid:

$$n_{\text{s}} \int_{z'<0} \mathrm{d}z' V_2(|\mathbf{r} - \mathbf{r}'|) \rightarrow -(\pi/6) n_{\text{s}} C_6/z^3. \tag{4}$$

Thus, in this two-body *approximation* $C_3 = (\pi/6) n_{\text{s}} C_6$ [13].

A rather different way to derive a z^{-3} power law is perhaps more intuitive, invoking the fundamental origin of VDW interactions. It is based on the fact that (even at zero temperature) any atom has a charge distribution that undergoes time-dependent, quantum-mechanical (zero-point) fluctuations. The resulting instantaneous dipole moment creates an image dipole inside the nearby surface, with which it has an instantaneous z^{-3} dipole–dipole electrostatic interaction, which is *always* attractive because of the correlation between the image and original dipoles; see Figure 1. Averaging over all such fluctuations yields the z^{-3} interaction. While this model is always correct, the former (integration or summation) model yields the correct answer only in the limit of negligible screening, as will follow from an exploration of the general behaviour of the coefficient C_3. The coefficient C_3 is given *rigorously* [14] by DLP theory, by integrating over all frequencies:[3]

$$C_3 = [\hbar/(4\pi)] \int \mathrm{d}\omega\, \alpha(\mathrm{i}\omega) g(\mathrm{i}\omega), \tag{5}$$

$$g(\mathrm{i}\omega) = [\varepsilon(\mathrm{i}\omega) - 1]/[\varepsilon(\mathrm{i}\omega) + 1]. \tag{6}$$

Equation (5) is an integral over positive frequencies $0 \leq \omega \leq \infty$ of a product of the polarisability of the molecule $\alpha(\mathrm{i}\omega)$ and the 'surface-response' function $g(\mathrm{i}\omega)$. The latter name is associated with the fact that the

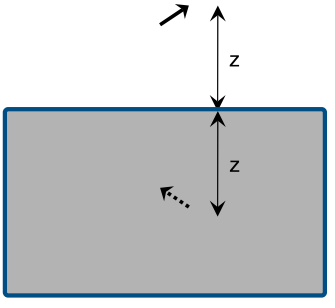

Figure 1. Schematic of an instantaneous, fluctuating dipole (solid arrow) on an atom outside a surface, and the corresponding image dipole (dashed arrow) within the solid.

electrostatic image [15] of a charge inside a surface, in response to a charge q outside the surface, is given by $q_{\text{image}} = -qg(\omega)$. In Equation (5), the functions $\varepsilon(i\omega)$ and $\alpha(i\omega)$ are evaluated at purely imaginary frequency, as indicated, but these functions can be determined from experimentally measured quantities at real frequency. For example, a Kramers–Kronig relation yields an expression for $\varepsilon(i\omega)$ in terms $\varepsilon_2(\omega)$, the absorptive part of the dielectric function at real frequency [16]:

$$\varepsilon(i\omega) - 1 = (2/\pi)\int d\omega'\, \omega' \varepsilon_2(\omega')/[\omega'^2 + \omega^2]. \quad (7)$$

There is no physical significance of an imaginary frequency; however, it enables a mathematical evaluation by complex variables theory. Moreover, it yields a convenient form of expression; without this transformation, Equation (5) would involve a double (or triple) integral. Note from the right side of Equation (7) that, since $\varepsilon_2 >= 0$, $\varepsilon(i\omega) - 1$ is a positive definite function which decreases with increasing ω.

A number of important points can be made about these various relations. One is that the VDW interaction is *completely quantum-mechanical* in origin. This can be seen in the proportionality of $V_{gs}(z)$ and C_3 to $\hbar$, which is zero in the classical limit, and the key role played by quantum fluctuations. Another important fact is that Equation (5) involves the dielectric function, a bulk property that embodies electrostatic screening. Thus, an atom within the solid experiences electric fields that are affected by the dipoles of the neighbouring atoms. This problem of screening is one that must be recognised when dealing with interactions involving dense media. In particular, one should not assume that two atoms which are surrounded by other atoms experience the same mutual interaction as when they are in vacuum. A final point is this: Equation (6) involves the bulk dielectric function. While the dielectric properties are altered near the surface, the preceding equations are based on the macroscopic continuum assumption, explaining why Equation (3) is really an asymptotic relation, which breaks down at small z. When the atom is at a *large* separation z, in contrast, the relevant fluctuating fields extend a comparably large distance $\sim z$ into the solid, so that the bulk approximation to ε is well-justified. This behaviour will be exemplified by numerical results presented in the following section. It is important to recognise that while the atomic polarisability of a material might be altered near an interface, especially for the case of strong covalent bonding, the dielectric function will surely be altered near the surface since it depends upon the atomic polarisability *and* the local arrangement of atoms.

We may further illuminate the nature of the integral in Equation (5) by considering two very different limiting cases. One *extreme* example involves the case of a *perfect* metal, for which $\varepsilon(i\omega) \rightarrow +\infty$. Then, the response function $g(i\omega) = 1$ (the image dipole has the same magnitude as the external dipole), so the interaction coefficient becomes

$$(C_3)_{\text{metal}} = [\hbar/(4\pi)]\int d\omega\, \alpha(i\omega). \quad (8)$$

The 'fluctuation–dissipation' relation applied to the electronic properties of matter yields an exact relationship between this integral and the mean-square dipole fluctuations of the atom, $\langle p^2 \rangle$ [17]. This relationship results in a remarkably simple final answer for this perfect metal case [18]

$$V_{gs}(z) = -\langle p^2 \rangle/(12z^3). \quad (9)$$

This equation has a very physical interpretation. The electrons of the atom exhibit quantum fluctuations of the charge, giving an instantaneous dipole. At any instant of time, the metal responds with a perfectly correlated image charge, located at the mirror image position, a distance z below the metal's surface; see Figure 1. The z^{-3} dependence in Equation (9) and the coefficient represent the time-averaged interaction between the atom's fluctuating dipole and its image. We note one more property of this perfect metal limit; it is manifestly not pairwise additive. If one were to increase the metal's density by, say, 25%, the potential does not change at all, while a pairwise additive potential would change by 25%.

There is another, important limit of Equation (5): the case of a weakly polarisable solid, i.e. $\varepsilon_{\text{weak}}(i\omega) - 1 \ll 1$; this is the *opposite* limit to the metal situation. In this case, denoted 'weak', we may express the solid's dielectric function in terms of n_s and the polarisability, $\alpha_s(i\omega)$, of the constituent atoms; using the Lorentz–Lorenz relation, which is a low-density version of the more general Clausius–Mossotti equation, one has

$$\varepsilon_{\text{weak}}(i\omega) - 1 \approx 4\pi n_s \alpha_s(i\omega). \quad (10)$$

In that limit, Equation (5) yields

$$(C_3)_{\text{weak}} \approx [\hbar n_s/2]\int d\omega\, \alpha(i\omega)\alpha_s(i\omega). \quad (11)$$

This expression and Equation (2) have a very simple interpretation, as one can see from Equations (3) and (4). The interaction (in this weakly polarisable limit) is precisely equal to the sum of all two-body interactions between the adsorbed atom and the atoms comprising the solid. This two-body interaction satisfies $V_2(r) = -C_6/r^6$, with the coefficient given by the quite general relation,

which is derived in Appendix A:

$$C_6 = [3\hbar/\pi]\int \mathrm{d}\omega\, \alpha(\mathrm{i}\omega)\alpha_s(\mathrm{i}\omega). \tag{12}$$

Note, in contrast, that the perfect metal involves complete screening of the interactions, yielding a very different result, Equation (8), from that (Equation (11)) for a weakly polarisable material where screening is negligible. The perfect metal case involves a collective response of the free electrons responsible for its metallic properties. This behaviour is not captured in a model based on individual atoms' properties.

What about intermediate cases between these extremes? Equations (5) and (6) permit an exact calculation. But instead of looking at this general case, one can do a Taylor expansion of the general relation Equation (5) in the difference, $\varepsilon(\mathrm{i}\omega) - 1$, yielding a many-body expansion: $C_3 = C_3^{(2)} + C_3^{(3)} + C_3^{(4)} + \cdots$ The successive terms represent two-body, three-body and higher order contributions to the VDW coefficient C_3. This sum-of-all-orders approach is implicit in some of the following discussion. It is derived explicitly in Appendix B where it is shown that the ratio of successive terms is of order $n_s\alpha_s$.

While the general Equation (5) may look forbidding, there are many convenient approximations which yield *analytic* expressions and these are often sufficiently accurate for most purposes. One description we will use frequently is the Drude approximation to the atom. This model was used by London in his pioneering studies of VDW interactions [10,19], and is still frequently employed for this purpose since it captures the key features of VDW interactions. In the simplest version of the model, the atom's dynamics are represented by the motion of a *single* electron, bound to the nucleus with a spring, with force constant $k = m\omega_0^2$, where ω_0 is a characteristic frequency. Then, the potential energy is $m(\omega_0\mathbf{r})^2/2$. The classical equation describing its motion in an electric field $E\exp(-\mathrm{i}\omega t)$ in the x direction is

$$m\mathrm{d}^2x/\mathrm{d}t^2 = -m\omega_0^2x - eE\exp(-\mathrm{i}\omega t). \tag{13}$$

The solution for the displacement, driven by the electric field E, is then $x(t) = eE\exp(-\mathrm{i}\omega t)/[m(\omega^2 - \omega_0^2)]$, so that the atomic polarisability is given by

$$\alpha(\omega) = e^2/[m(\omega_0^2 - \omega^2)]. \tag{14}$$

Hence, the corresponding value at imaginary frequency (needed for the VDW relations) may be written

$$\alpha(\mathrm{i}\omega) = \alpha_0/(1 + \omega^2/\omega_0^2), \tag{15}$$

$$\alpha_0 = e^2/(m\omega_0^2). \tag{16}$$

With SI units, one needs to divide the right hand side by $4\pi\varepsilon_0$. Inputting typical values, including $e = 1.6 \times 10^{-19}$ C, $m = 9.1 \times 10^{-31}$ kg, and $\omega_0 = 3 \times 10^{16}\,\mathrm{s}^{-1}$ gives $\alpha_0 = 3.0A^3$. With Equations (12) and (15), one obtains from perturbation theory the *London formula* for C_6:

$$C_6 = (3/4)\hbar\omega_0\alpha_0^2. \tag{17}$$

Appendix A explains the remarkable fact that this semi-classical treatment *coincides* with that of the fully quantum treatment of electronic response, within the framework of the assumed harmonic model of the electronic potential. To evaluate Equation (17) for a given atom requires a specification of its characteristic energy, $\hbar\omega_0$; this quantity is sometimes taken to be the ionisation energy I of the atom. Alternatively, Equation (17) may be used to determine the energy from known values of α_0 and C_6. The resulting value of $\hbar\omega_0$ is about 20% above the value of I for inert gas atoms and saturated molecules, while for alkali and alkaline earth metal atoms the result is considerably less than I. Appendix C presents these results and an assessment of the reliability of the single-frequency Drude model for treating VDW interactions. In about 75% of the 22 cases tested, the result for C_6 falls within 5% of the exact value, while in the other cases there is an error as large as 11%. For some applications, these errors are acceptable because other aspects of the problem present comparable, or larger, uncertainties.

A similar, simplifying approach to computing the C_3 dispersion coefficient involves the surface response function, which may be modelled by a fitting function $g(\mathrm{i}\omega)$:

$$g(\mathrm{i}\omega) = g_0/(1 + \omega^2/\omega_s^2). \tag{18}$$

Indeed, such an expression is *exact* for both a weak polarisability solid and a free electron metal. The latter case can be seen from recognising that such a metal's dielectric function can be written as $\varepsilon(\omega) = 1 - \omega_p^2/\omega^2$, expressed in terms of its plasma frequency ω_p. This quantity satisfies $\omega_p^2 = n_s e^2/m\varepsilon_0$, where n_s is the number density of the atoms in the material. We then have

$$\varepsilon(\mathrm{i}\omega) = 1 + \omega_p^2/\omega^2. \tag{19}$$

Note that Equation (18) results with $g_0 = 1$ if one takes $\omega_s = \omega_p/\sqrt{2}$, which is the surface plasmon frequency for a half-space metal bounded by the $z = 0$ plane. That finding is consistent with the description of $g(\mathrm{i}\omega)$ as the surface response function, since the surface plasmon is the normal mode of the surface of a metal, manifested experimentally in electron energy loss experiments in thin films. Equation (19) is a good approximation for free electron metals, like *Al* and alkali metals. Fits to real dielectric data yield $g_0 \sim 0.98$ for such materials. For other materials, including semiconductors, noble metals

and insulators, fits yield much smaller values of g_0 than 1, reflecting the relatively weaker dielectric response [20].

If one uses the two parameterisations, Equations (15) and (18), in Equation (5), one arrives at a simple result for the dispersion coefficient for the gas-surface interaction coefficient:

$$C_3 = (g_0\alpha_0\hbar\omega_s/8)(1 + \omega_s/\omega_0)^{-1}. \tag{20}$$

This expression for C_3 yields both limiting cases discussed previously. For example, the perfect metal corresponds to setting $g_0 = 1$ and assuming an 'instantaneous' response of the metal compared to that of the atoms, i.e. $\omega_s/\omega_0 \gg 1$.

For more complex geometries, one of the most commonly used approaches to treating VDW interactions was introduced by Hamaker [9]. In this approach, the usual starting point is the coefficient A of the nonretarded VDW interaction energy per unit area $V_{\text{half-half}}(z)$ between two half-spaces, bounded by parallel faces separated by distance z:

$$V_{\text{half-half}}(z) = -A/(12\pi z^2). \tag{21}$$

The coefficient A is computed 'exactly' from the frequency-dependent dielectric functions of the interacting media. Now, suppose instead that this interaction could be evaluated from the interatomic interaction $V(r) \sim -C_{AB}/r^6$ between atoms of the two bodies, made of atomic species A and B. The result of a double integration over the two bodies (of atomic number densities n_A and n_B) would be an expression of the preceding form, with a coefficient given by

$$A_{\text{pair}} = \pi^2 n_A n_B C_{AB}. \tag{22}$$

Hamaker's procedure is to use this relation to evaluate the pair interaction coefficient C_{AB} from the (nominally) exact coefficient A, derived from the full, many-body treatment of interacting half-spaces; that is

$$C_{6,\text{Hamaker}} \equiv \frac{A}{\pi^2 n_A n_B}. \tag{23}$$

While this approach is exact when the geometry is, in fact, two half-spaces, it gives a misleading result for other geometries since it actually over-corrects for screening. One does not know, in general, how reliable this method is. In those many cases when the geometries are not ideal enough to know A from DLP theory, we are thus *not* able to obtain accurate results by using the pairwise additivity, or Hamaker, approach. For these nanoscale situations, we need an approach that allows the discrete placement of atoms, as the pairwise additivity approach does, and yet which captures the many-body interactions, as DLP theory does. The CDM captures both aspects exactly, as discussed in the next section. Knowing this result permits one to assess the Hamaker, or other, approximations.

In the preceding discussion, we have pointed out limitations associated with the common assumption that VDW interactions are pairwise additive. A dramatic example involves the case of a metal surface, discussed above where many-body effects are expected. However, there are some quite different situations that also reveal the problems inherent in this assumption, even though these difficulties might not have been anticipated. We briefly mention two of these. In one geometry, we consider an atom (A) interacting with two distant, atoms, B and C, which we call a dimer. B and C are closely-spaced. The A-dimer interaction would be twice the A–B interaction if many-body forces were omitted. Let us evaluate the error in this two-body estimate. The vector $\boldsymbol{\delta}$ connecting atom B to atom C is oriented at angle θ relative to the vector $\mathbf{r}$ connecting the dimer's centre to atom A and $|\boldsymbol{\delta}| \ll |\mathbf{r}|$. In the case of all identical species, the r^{-6} interaction coefficient between A and the BC dimer satisfies [3]

$$C_6(\theta) = 2C_{AB}\{1 + \gamma(1 - 3\cos^2\theta/2)], \tag{24}$$

$$\gamma = 2(\alpha_\parallel - \alpha_\perp)/[3(\alpha_\parallel + \alpha_\perp)]. \tag{25}$$

Here, C_{AB} is the VDW coefficient for a single AB interaction, in the absence of atom C. The failure of additivity appears whenever the γ parameter is non-vanishing, meaning that the dimer is anisotropic. How large is this parameter? In the case of the Drude model, we have for a dimer [21]

$$\alpha_\parallel/\alpha_\perp = (1 + 2\psi)/(1 - 2\psi), \tag{26}$$

$$\psi = \alpha_0/r^3. \tag{27}$$

Thus, the failure of additivity depends on the molecular analogue of the parameter ν used to describe many-body effects in bulk materials. We define the parameter $\nu = n\alpha$, which is the number density (n) of the material (e.g. $1/n$ given by the cube of the lattice constant, a^3) and the material polarisability (α). In a 'typical' case, $\nu \sim 0.1$, so the anisotropy parameter γ is also comparable to 0.1 [22].

The second geometry we consider involves a similar dimer, placed near a perfect metal surface. Harris and Feibelman [23] showed that the z^{-3} interaction coefficient has an isotropic piece, $C_3^{(0)}$ (dependent on the average polarisability), plus an orientation-dependent part:

$$C_3 = C_3^{(0)} + C_3^{(2)}P_2(\cos\theta). \tag{28}$$

Here, $P_2(x)$ is the second Legendre polynomial and θ is the dimer axis's orientation relative to the surface-normal. The coefficient

$$C_3^{(2)} = [\hbar/(4\pi)]\int \mathrm{d}\omega\, \Delta\alpha(\mathrm{i}\omega)g(\mathrm{i}\omega). \tag{29}$$

The difference $\Delta\alpha = \alpha_{\|} - \alpha_{\perp}$. Thus, the behaviour is qualitatively similar to that in the preceding problem; the molecule–surface interaction energy is not twice that of the independent atoms, but there is an orientation-dependent piece which manifests the many-body (here, two-body) effect. Calculations of this dependence have been reported [24]. In the case of a weakly anisotropic molecule, the effect is small ($C_3^{(2)}/C_3^{(0)} \sim 0.05$ for H_2), but it is larger for more anisotropic molecules.

The preceding discussion *assumes* the validity of electrostatics in describing the VDW energy arising from coupled dipole motions. However, at very large separation between the interacting bodies, electrostatics fail because the bodies are so far apart that the coupled motions of interacting dipoles become imperfectly correlated, due to the time delay associated with the finite speed of light. Consequently, the range of distance L where this *retardation* can be ignored is limited to a so-called *nonretarded* regime, $L \ll L_{\text{nonretard}}$. Its extent can be crudely estimated in terms of the distance travelled by light during an electronic period of vibration within an atom: $L_{\text{nonretard}} \sim c/\omega \sim c\hbar/\Delta E$, where the uncertainty principle has been used to estimate the characteristic frequency ω from the electronic level spacing ΔE. Identifying $\Delta E \sim 10\,\text{eV}$, for example, yields $L_{\text{nonretard}} \sim 20\,\text{nm}$. This highly simplified estimate turns out to be relatively accurate, at least for half spaces (Figure 2); VDW interactions involving surfaces are typically reduced to about one-half of their nonretarded values when the separation becomes about 20 nm. We will explain in Section 4 why retardation is less significant for the interaction between two atoms. In the opposite regime, $L \gg L_{\text{nonretard}}$, the VDW interaction is said to be *fully retarded*. Then, for example, the gas-surface interaction assumes a rather different form: $V_{\text{retard}}(z) \sim -C_4/z^4$, where the coefficient [25]

$$C_4 = [3\hbar c\alpha_0/(8\pi)]\phi_{\text{ad}}(\varepsilon_1)\{[\varepsilon_s(0) - 1]/[\varepsilon_s(0) + 1]\}. \tag{30}$$

Here, $\phi_{\text{ad}}(\varepsilon_1)$ is a slowly varying function of the static dielectric function of the solid ε_1. Note that this z^{-4} power law differs from that (z^{-3}) of the nonretarded interaction and that this coefficient C_4 depends on just the *static* polarisability of the atom and the *static* response function of the surface. For weak atomic polarisabilities and isotropic materials, a similar r^{-7} power law and C_7 coefficient exists to describe fully retarded interactions.

As seen in Figure 2, the nonretarded description is applicable only to distance scales of order a few nm, or less, since the effects of retardation are $<10\%$ of the full interaction only at distances $<2\,\text{nm}$. For larger separations, the time required for the electromagnetic field to traverse the distance from one atom to another and back becomes comparable to the time required for the electron distribution of the first atom to change. Thus, the degree of correlation – and therefore attraction – decreases. In the *fully retarded* regime, this distance becomes so large that only the static frequency response is relevant. The fully retarded regime corresponds to separations $\geq 0.1\,\mu\text{m}$. Between these two regimes lie an extended intermediate distance regime, say 2–100 nm. Between two 10 nm silica particles in a vacuum medium, the VDW interactions will be $<1\,kT$ at 5 nm separation, while for 1000 nm silica particles in vacuum the attraction will be tens of kT.

It is important to note that this paper is concerned *exclusively* with the asymptotic interaction. For the interatomic potential, the long-range interaction C_6/r^6 is the dominant (nonretarded) term at large separation, but corrections to this term are needed as r approaches the equilibrium separation of the atoms. These corrections, beyond the scope of this paper, include damping of this (dipole–dipole) term and the addition of higher order multipole interactions (dipole–quadrupole, etc.) of the form C_{2n}/r^{2n}, where $n = 3$, 4, 5, and beyond [27]. The values of these coefficients have been calculated accurately for the first few n values from the respective frequency-dependent polarisabilities (e.g. dipole, quadrupole) [28–30].

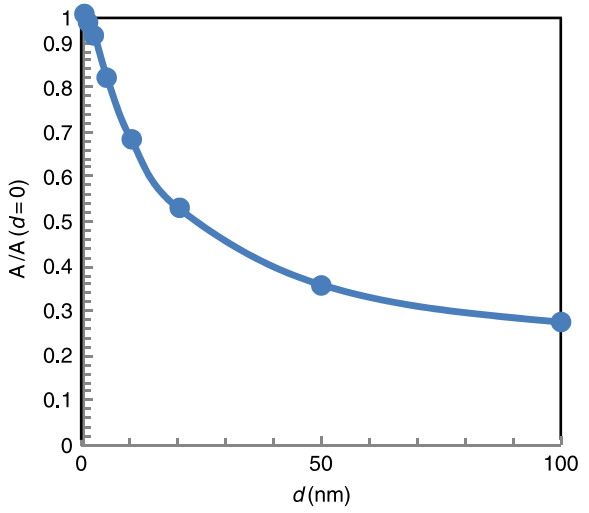

Figure 2. The reduction in effective Hamaker constant due to retardation. The Hamaker constants are calculated from the literature [26], and a reduction to half the zero-separation value is common at $d = 20\,\text{nm}$. The curve is shown for two half spaces of polystyrene across water, at 10^{-7} M ions (i.e. below that of water in equilibrium with CO_2). Retardation sets in even at close separations, such as $d = 1\,\text{nm}$. Interestingly, a broad range of materials demonstrate a similar behaviour, including silica across water, and graphite or even gold across vacuum.

3. The CDM for nanoscale VDW energies

The CDM evaluates the VDW energy from the spectrum of collective motions of the ensemble of electric dipoles,

one at each atomic position, which fluctuate in the presence of their mutual interactions. Thus, the method captures the complete 'dipole conversation' in the system, which is the essence of the many-body effects. In the model, we approximate that each electron obeys the classical motion embodied in the Drude model described earlier, although this is not a strict requirement of the technique. In the Drude model, two parameters, a static polarisability (α_0) and a resonant frequency (ω_0), characterise the electron's dynamics within an atom. The atom's dipole interacts with all other instantaneous dipoles by classical electrostatic dipole interactions. The eigenfrequencies $\{\omega_i\}$ of the resulting collective electron motions provide the zero-point energies, $\{\hbar\omega_i/2\}$. The total VDW energy is the sum, over the 3N normal modes, of these energies. Then the VDW interaction energy, V_{int}, is given by the difference between this sum and the energy of this collection of the N atoms when they are infinitely far apart:

$$V_{\text{int}} = \Sigma_i\{\hbar\omega_i/2\} - 3N(\hbar\omega_0/2). \qquad (31)$$

The quantity $3\hbar\omega_0/2$ is the energy per atom of each isolated three-dimensional harmonic oscillator. Appendix A explains why this apparently classical description of the system's oscillations works *exactly* in solving the quantum-mechanical interaction problem for every such coupled dipole problem. This wonderful fact explains the utility of this method.

VDW interactions have been extensively studied for inert gases and simple saturated molecules (like CH_4), since these interactions are relatively simple to understand theoretically and explore experimentally. In particular, because of the weakness of their interactions, these particles are only weakly perturbed by their environment; hence, abundant gas-phase information exists concerning the properties of individual particles (e.g. polarisability) and their two-body interaction potentials. As discussed previously, pair interaction results are often assumed to be transferable to condensed systems. In some cases, corrections to this approximation have been calculated by adding three-body interactions. However, for more strongly interacting systems – that is, for higher values of $\nu \equiv \alpha_0/a^3$ – the neglect of higher than third order terms can result in a large error. One interesting finding, shown below in Figure 3, is that for an infinite line of atoms for all $\nu > 0.10$, while the three-body contribution is at most 2% of the two-body contribution, the total contribution of higher order terms (i.e. beyond three-body) exceeds the three-body term, and indeed becomes comparable to two-body terms. Thus, *a small magnitude of the three-body term implies neither that higher order terms are individually small or that they mutually cancel*. We note in passing that Figure 3 reveals a limitation in the CDM which is inherent. Above a critical value ($\nu \sim 0.208$ for the one-dimensional chain), no solution exists. For such large ν values, the system is unstable, because (at long wavelength) the force provided by the local field (due to the surrounding dipoles) exceeds the spring restoring force.

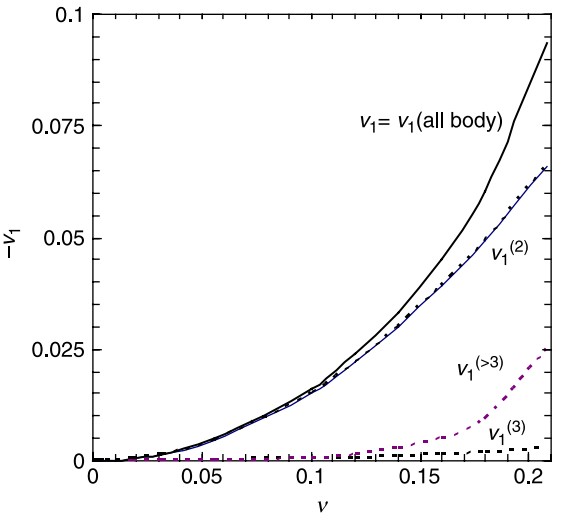

Figure 3. The dimensionless energy per atom (v_1) of an infinite line of atoms. The full (all body) calculation for v_1 was done with the CDM. For all values of ν, even up to the critical value of 0.208, the three-body contribution per atom ($v_1^{(3)}$) is small, while higher order interactions ($v_1^{(>3)}$) cannot be neglected.

The CDM has been used for decades. Bade and Kirkwood [31] used an identical method to evaluate dispersion forces for a linear lattice in 1957. [31] arose from the recognition from even earlier works, including by London, that by putting the quantum aspects of the dispersion forces into atomic polarisabilities and using the energy of a harmonic oscillator, one could obtain 'proper frequencies' [32], and as a result, dispersion energies [33].

Variants of the CDM have been used previously by a number of groups. Lucas and co-workers [34–37] used the CDM to evaluate the VDW energy of infinite two and three-dimensional systems. Girard and Bouju [38] examined dispersion forces for atomic force microscope tips. Our own group has studied a variety of finite cluster systems [39,40]. Each problem involves a common expansion parameter (ν). [31] calls this parameter β, and it has other designations elsewhere. An expansion of the interaction energy, V, leads to the two-body interaction term (V_2, proportional to ν^2), the three-body energy term (V_3, proportional to ν^3), and so on. These results coincide with the sum of two-body and three-body interaction energies. Elements of the CDM method have been used previously in the light scattering and other literature [41,42], in addition to its use in assessing VDW forces.

In using the CDM to calculate VDW forces, we examine two clusters A and B. Each cluster contains a number of atoms, N_A and N_B, and each of these atoms will

have a dipole ($\mathbf{p}_i$) in an electric field ($\mathbf{E}$) that is given by

$$\mathbf{p}_i = \alpha_i \mathbf{E}(\mathbf{x}_i). \tag{32}$$

The local electric field consists of an applied field ($\mathbf{E}_0$) as well as the fields resulting from the instantaneous dipoles ($\mathbf{p}_j$) of all other atoms in the system. That is,

$$\mathbf{E}(\mathbf{x}_i) = \mathbf{E}_0 + \sum\nolimits_{j=1,j\neq i}^{N_A+N_B} \mathbf{T}_{ij}\mathbf{p}_j, \tag{33}$$

where the interaction tensor $\mathbf{T}_{ij} \equiv \left(3\mathbf{n}_{ij}\mathbf{n}_{ij} - \mathbf{I}\right)/r_{ij}^3$ for $i \neq j$ and $\mathbf{T}_{ij} = \mathbf{0}$ for $i = j$. In these equations $\mathbf{n}_{ij}$ is the unit normal vector between atoms i and j; $\mathbf{I}$ is the 3D identity tensor; and r_{ij} is the distance between atoms i and j. We now have a set of self-consistent coupled equations for the dipoles, for each i from 1 to $(N_\mathrm{A} + N_\mathrm{B})$ in both clusters:

$$\frac{\mathbf{p}_i}{\alpha_i} - \sum_{j=1}^{N_A+N_B} \mathbf{T}_{ij}\mathbf{p}_j = \mathbf{E}_0. \tag{34}$$

We can then define a $(3N_\mathrm{A} + 3N_\mathrm{B}) \times (3N_\mathrm{A} + 3N_\mathrm{B})$ matrix $\mathbf{Q}$ of interactions and a $(3N_\mathrm{A} + 3N_\mathrm{B})$ column vector ($\mathbf{P}$) of dipoles such that $Q_{3(i-1)+k,3(j-1)+m} = -T_{ij}^{(km)} + \delta_{km}/\alpha_i$ and $P_{3(i-1)+m} = p_i^{(m)}$, involving the (km) component of the ij interaction tensor ($\mathbf{T}$) and the Kronecker delta function (δ_{km}), where k or $m = 1, 2, 3$ for the x, y, or z component of a vector, respectively. Since the VDW forces exist even when $\mathbf{E}_0 = \mathbf{0}$, we can write $\mathbf{Q}\cdot\mathbf{P} = \mathbf{0}$. The equation has a trivial solution $\mathbf{P} = \mathbf{0}$, but it also has a solution when $\det \mathbf{Q}(\omega) = 0$. Thus, we can find all the values of ω that give $\det \mathbf{Q} = 0$. Finding these normal mode frequencies is the heart of the CDM, and the normal modes enable us eventually to evaluate the VDW interaction.

In principle, we can use any model for the atomic polarisability, but, as discussed previously, we often use the Drude model. Furthermore, we could use a superposition of Drude oscillators for each atom to account for several resonant frequencies, at the expense of a longer computational time, but one often finds that a single ultraviolet contribution to the VDW forces dominates other resonant frequency contributions for an atom. Setting $\mathbf{E}_0 = \mathbf{0}$ and substituting the Drude model into Equation (34) gives $\omega_{0i}^2\mathbf{p}_i - \omega^2\mathbf{p}_i = \alpha_{0i}\omega_{0i}^2\sum_{j=1,j\neq i}^{N_A+N_B}\mathbf{T}_{ij}\mathbf{p}_j$, and by defining $\Omega_{3(i-1)+k,3(j-1)+m} = -\alpha_{0i}\omega_{0i}^2 T_{ij}^{(km)} + \omega_{0i}^2\delta_{ij}\delta_{km}$ for the km component of the ij interaction, we obtain $\Omega\cdot\mathbf{P} = \omega^2\mathbf{P}$.

Standard algorithms can be used to solve this eigenvalue problem. Each eigenvalue represents the square of a normal mode frequency (ω^2). Since, each frequency contributes $\hbar\omega/2$ of energy (or at finite temperature, $\hbar\omega/2\coth(\hbar\omega/2kT)$), we can find the energies for the isolated clusters A and B, and also for the combined system of cluster A near cluster B. Taking the difference between the energy of the complete system and that of the two independent clusters gives the 'exact' interaction energy, subject only to the assumptions that the Drude model describes the atomic polarisabilities, that only dipole interactions are important, and that retardation is not important. The CDM automatically provides the contributions of all n-body forces, computed explicitly, which is unusual in condensed-matter physics. The CDM gives results that are entirely consistent with DLP theory in those regimes of large separation and simple geometry for which the DLP assumptions are plausible, but not at close approach or for irregular bodies, in which case the DLP model is not relevant.

What about higher order multipole interactions, such as dipole–quadrupole or quadrupole–quadrupole? While the higher-order multipoles may play an important role for neighbouring atoms, and therefore, intracluster interactions or cohesion problems, quadrupole–dipole and other higher order interactions play a small role when the intercluster atom–atom distances are large compared with the size of the atoms, such as for VDW energies. Furthermore, since the VDW energy is the difference in the calculated energies of the total system and of the two isolated clusters, any errors in the intracluster energies are subtracted out.

We (and many others) have previously used the Axilrod–Teller–Muto (ATM) approach to calculate the first correction to the two-body sum [43–45]. However, the ATM approach neglects four-body corrections and higher, which can be important. In fact, as shown in both the preceding example and Figure 4, the addition of only a

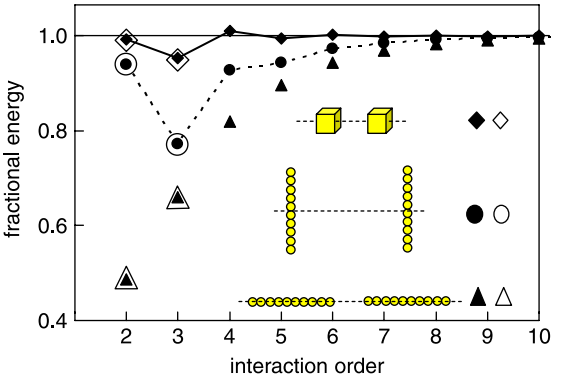

Figure 4. Fraction of total VDW interaction energy, as a function of the highest order of many-body terms included [39]. Triangles (circles) correspond to the configurations shown for two 10-mers at separation $r/a = 50$. Diamonds correspond to 27 atom cubic clusters at $r/a = 10$. Dashed and solid curves are drawn to guide the eye. The closed symbols are from the full CDM, while the open symbols are directly from the summation of two- and three-body interactions. For these calculations, $\omega_0 = 2.033 \times 10^{16}$ rad/s and $n_\mathrm{s}\alpha_0 = 0.115$, where n_s is the bulk atomic density.

three-body force is often misleading, giving a result that has a *greater* error than the simple two-body summation.

In general, many body interactions are less important for symmetric shapes than for non-symmetric shapes, as shown in Figure 4, presenting results for large separations ($r \gg$ lattice constant a). Note that the two-body interactions capture the essence of the energy for the cubes. The inclusion of three-body interactions for cubes actually makes the predictions VDW *less accurate*. However, the inclusion of higher-order corrections shows that three-body and higher-body interactions essentially cancel for the symmetric cubes. In contrast, for the asymmetric chains, especially where the chains are co-linear, we see that all higher-order interactions are of the same sign and lead to a large contribution, with no cancellation. Presumably, the relatively common belief that higher-order interactions cancel is based on some calculations for symmetric shapes, but it is not correct in general. For nanoscale systems – which often contain sharp corners or other rough features compared with the size scale of the particles – careful calculations are necessary and the CDM is the tool of choice.

It is comforting to note, however, that for symmetric shapes, the CDM reduces to known Lifshitz results for spheres, as shown in Figure 5. We see that at large interparticle separations, the CDM gives the same results as Lifshitz theory for spheres, as given by Langbein [46], as expected. However, as the separation between particles diminishes, continuum theories – whether the Langbein solution or the Hamaker approach – diverge, giving unphysically large results. In contrast, the discrete two-body sums give results within 10 or 20% of the CDM. The two-body sum depends on how the coefficient describing the VDW interaction between two particles is calculated, whether based on two atoms or on macroscopic bodies à la Hamaker. When C_6 is obtained by fitting VDW interactions to macroscopic results for geometries other than spheres, the inclusion of screening is over-corrected for, still yielding an error. We note that the Derjaguin approximation over-predicts the VDW attraction by at least five times. Thus, this commonly-used estimation method gives a prediction for the VDW energies that would usually be regarded as quite inadequate.

As mentioned in connection to Figure 4, one limitation of the CDM involves materials with large polarisability densities, $\nu = n_s\alpha$. A well-known 'polarisation catastrophe' occurs mathematically [47]. When ν exceeds some value, which we call ν_{crit}, imaginary eigenfrequencies result, from which VDW energies can no longer be calculated; this means that the system assumed in the calculation is unstable. The value of ν_{crit}, depends on the geometry of the cluster, as well as its size. This is shown, for instance, in Figure 6. Even for one dimension, a shorter chain allows a higher coupling parameter than an infinite chain. For three dimensions, $\nu_{crit} = 3/4\pi \approx 0.239$. This is an important

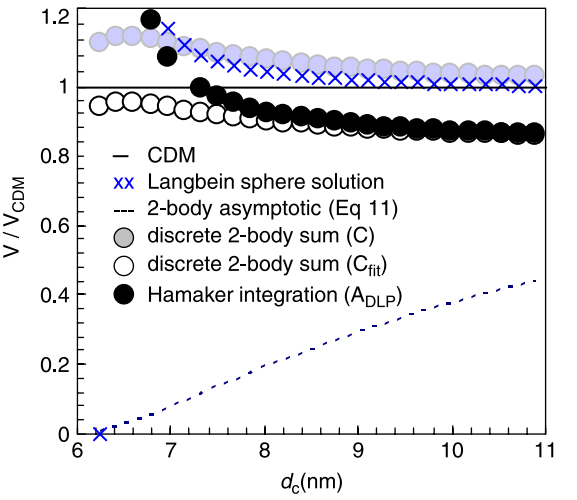

Figure 5. Ratio of various methods for computing VDW forces to the exact CDM method, for two identical spheres with $N = 2340$ atoms in each. The centre-to-centre distance between the spheres (d_c) is the same for both the continuum and discrete methods. The cluster diameters are both 5.88 nm. Due to the discrete placement of the atoms within the cluster, analytical methods (e.g. Langbein, Hamaker) far over-estimate the result for small gaps, although the Langbein result is within 2% when the gap is 3 nm. The two-body sum with C approaches the exact CDM value at far distances, since multi-body effects essentially disappear. At much larger separations than shown on the figure, the CDM and Lifshitz theory converge to the same result, as expected. At far distances, the use of C_{fit} predicts a VDW interaction that is smaller than the exact value. Results from the Derjaguin approximation are far off this figure for the parameters listed; typically it overestimates V by a factor of five or more.

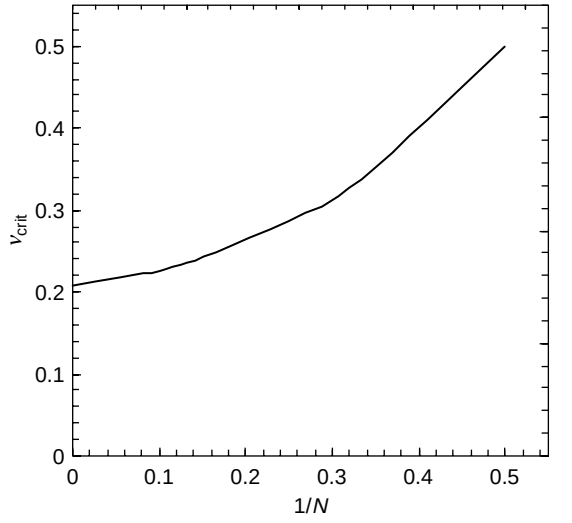

Figure 6. Critical coupling parameter (ν_{crit}) for chains of a finite number (N) of atoms. Note that the x-axis is $1/N$. Figure is from [21].

example where nanoscale effects – that is, neither atomic scale nor macroscopic scale – enter the physics.

4. Effects of retardation

The fully retarded interaction is sometimes called the 'Casimir interaction', because it was originally derived by Casimir (and Polder) in the late 1940s for a variety of geometries: between two neutral atoms, between a neutral atom and a metallic plane and between two metallic planes [25,48]. Their derivation is instructive, providing the basic idea even if it is restricted in its validity. For example, they determined the force between two metallic plates by evaluating the zero-point energy of the electromagnetic field between the plates (by summing over the discrete spectrum restricted by the boundary conditions) and by subtracting the corresponding zero-point energy for the plates at infinite separation (by replacing summation over discrete spectra with integration over continuous spectra in an infinite empty space). It is important to note that this energy for any separation is itself infinity, since the spectrum includes infinitely many modes, each of which has a finite zero-point energy, resulting in an ultraviolet divergence; nevertheless the result of looking at the difference (between infinite results) is well-defined. Indeed, the Casimir force has by now been amply confirmed by experiment. Recently, there has been considerable work done on the sign and magnitude of this force [49], for systems with various dielectric properties, stimulated by its importance in nanotechnology, like nanomechanical devices (NEMS), which are outside the scope of this article. For a complete review of the Casimir force between two planes, see the recent review article by Lamoreaux [12].

It is interesting to note that although Casimir and Polder used quantum field theory in their derivation of the interaction between two atoms, the result has been confirmed by a number of authors using different methods. For example, Aub et al. [50] obtained the same result by using quantum-mechanical perturbation theory. This semiclassical approach is relatively simple since it avoids the calculation of terms arising from a large number of Feynman diagrams. Also, McLone and Power [51,52] used quantum field techniques to calculate the interaction between two atoms (one in an excited and the other in the ground states), while Meath and Hirschfelder [53] derived the same expression with a semi-classical procedure. Lucas [35,36] used quantum field theory to evaluate the small radiative corrections to the nonretarded VDW cohesion energy of rare gas solids.

The Casimir–Polder expression for the interatomic potential is valid for all separations, but its evaluation requires an infinite summation over excited atomic states. There is no simple analytic equation for calculating the VDW force at all separations, which would be very useful in computer simulation studies. However, the result assumes a *universal*, albeit complicated, form within the Drude model, when the distance is expressed in terms of the characteristic wavelength $L_{\text{retarded}} = c/\omega_0 = \lambda\!\!\!^{-}_0$, discussed in Section 2. The result in this case appears in Figure 7, expressed as the 'retardation function' $G(r)$, defined by this relation [3,25,53]:

$$U(r) \equiv -G(r)C_6/r^6. \tag{35}$$

Thus, $G(r)$ modifies the nonretarded interaction so as to yield the 'true' interaction. One observes in this figure, as in Figure 2 for the half-space interaction, that the effect of retardation begins immediately, even at small r, becoming a correction factor 1/2; at a distance $r_{1/2} \sim 3\ \lambda\!\!\!^{-}_0$. For the case of atoms with characteristic energy $\hbar/\omega_0 = 10\,\text{eV}$, this yields $r_{1/2} = 60\,\text{nm}$. This distance is a factor of three larger than the value 20 nm seen in both Figure 2 for interacting half-spaces and what has been found for retarded gas-surface interactions [25,54]. The factor of three difference can be understood by recognising that the integration of interactions over solid bodies emphasise larger distance scales than the minimum separation, so that retardation sets in at a significantly smaller separation distance than is found for the interatomic problem [55]. Note, furthermore, that the nonretarded force is not correct even in the (formal) limit of zero separation, since this force includes the derivative of $G(r)$ with respect to r, which is nonzero.

The fully-retarded, asymptotic form of the interatomic interaction is

$$U(r) \sim -C_7/r^7. \tag{36}$$

This equation is seen in Figure 7 to agree with the general result when r exceeds $12\lambda\!\!\!^{-}_0$. For identical atoms, the

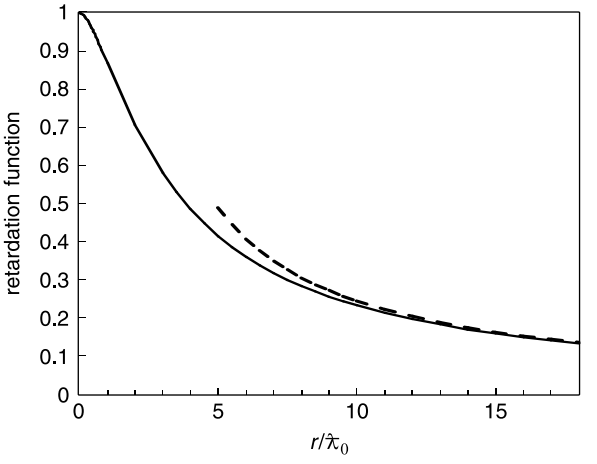

Figure 7. Retardation function $G(r)$, for identical neutral atoms at $T = 0$. This is a universal function of reduced distance r/λ_0. The values are from the tables in Meath and Hirschfelder [53]. Inset shows region of small separation. The dashed curve represents the fully retarded interaction, Equation (38).

coefficient

$$C_7 = [23\hbar c/(4\pi)]\alpha^2. \quad (37)$$

By comparing these expressions, one sees that the asymptotic form

$$G(r) \rightarrow [23/(3\pi)](\lambda 0/r). \quad (38)$$

We note that since $dG(0)/dr < 0$, the force, since it is the gradient of the potential, will be affected by retardation even for $r = 0$. However, the magnitude of the effect is small for $r < 1$ nm.

We now address the fully-retarded VDW interaction between two clusters at large separation where only static polarisabilities are important since all nonzero frequency response is asymptotically eliminated by retardation. The first method one might adopt would be to carry out a two-body pairwise summation using the fully retarded interatomic interaction $-C_7/r^7$, perhaps adding a three-body contribution as a single many-body correction [56,57]. As demonstrated in the previous section's discussion of the nonretarded VDW interaction between clusters, this approach is expected to be inaccurate, in general, since it may either over-estimate or under-estimate (depending on geometry) the many-body interaction.

An alternative strategy, which is *exact,* in that it includes all many-body terms, is to determine the static polarisability tensor of each cluster, using the CDM, and substitute it into the generalised expression for the fully retarded interaction between two atoms, including the anisotropic polarisability [56–58]:

$$V^{(2)}_{\text{aniso}} = -\frac{\hbar c}{8\pi}\frac{\aleph(A:B)}{{r_{AB}}^7}, \quad (39)$$

where

$$\begin{aligned}\aleph(\text{A}:\text{B}) &= 13\left[\alpha^{(\text{A})}_{11}\alpha^{(\text{B})}_{11} + \alpha^{(\text{A})}_{22}\alpha^{(\text{B})}_{22}\right] + 20\alpha^{(\text{A})}_{33}\alpha^{(\text{B})}_{33} \\ &\quad + 26\alpha^{(\text{A})}_{12}\alpha^{(\text{B})}_{12} - 30\left[\alpha^{(\text{A})}_{23}\alpha^{(\text{B})}_{23} + \alpha^{(\text{A})}_{31}\alpha^{(\text{B})}_{31}\right]. \quad (40)\end{aligned}$$

Here, $\alpha^{\text{A(B)}}_{jk}$ is the polarisability tensor of atoms (clusters) A(B), with the index 3 indicating the direction along the line connecting the two particles and the indices 1 and 2 referring to the perpendicular directions. This method treats each cluster as a (structured) point particle, which is clearly valid in the limit of very large separation, appropriate to the fully retarded regime. The static polarisabilities in some cases are known experimentally, but for small non-metallic clusters they may be calculated using the CDM. The result is an anisotropic polarisability tensor, in general, which depends strongly on the microscopic structure of the cluster. The surface effects due to the non-uniform local field near a surface or edge are shown to be significant, as exemplified in Figure 8 [59]. Note that, if one was to use the pairwise sum method to calculate the interaction, the corresponding polarisability distribution would be independent, isolated and uniform atomic polarisabilities, with no surface effect. As a result, the interaction would be (incorrectly) independent of the polarisation anisotropy in this large distance limit [57].

A comparison of these CDM-based results with those from the pairwise sum method reveals that the many-body interaction terms are significant: the higher-than-three body contribution to the interactions is always attractive and can be as high as 42% of the two-body sum [57]. In that study, we presented a power law expansion of the fully retarded VDW interaction as a series of n-body interaction terms. The results for interacting monolayer square clusters are shown in Figure 9.

Here, the 'fractional energy' is defined as the ratio of the energy, including many-body terms up to the specified interaction order, to the total energy. Just as was found in the previous section for nonretarded interactions, the fully retarded VDW interaction exhibits a strong dependence on the relative orientation of the anisotropic clusters even at infinite separation.

Unlike the case of nonretarded interactions (where the higher-order multipole interaction contributions cancel), the omitted contribution remains. Future investigation on the effect of these higher order multipole moments would be of great interest. The alert reader will note one further distinction between the retardation functions shown in Figures 2 and 7. While the former asymptotes to a constant

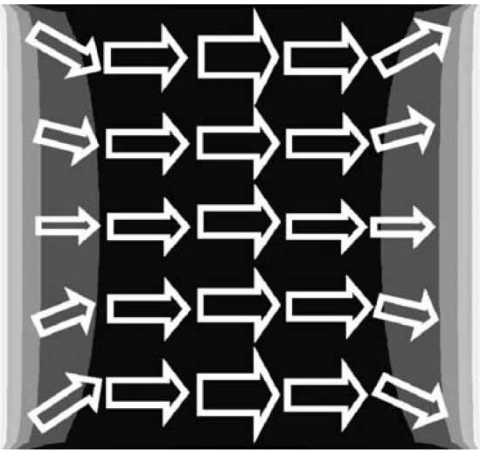

Figure 8. Magnitude distribution of the induced dipole moments in a square silica monolayer (60 × 60) when its surface is perpendicular to the external field, which points to the right in this figure. Darker (blue online) region implies a larger magnitude dipole. The local orientation and magnitude of dipoles are drawn with arrows. Taken from [59], which presents numerical values. © 2005; reproduced by permission of the American Physical Society.

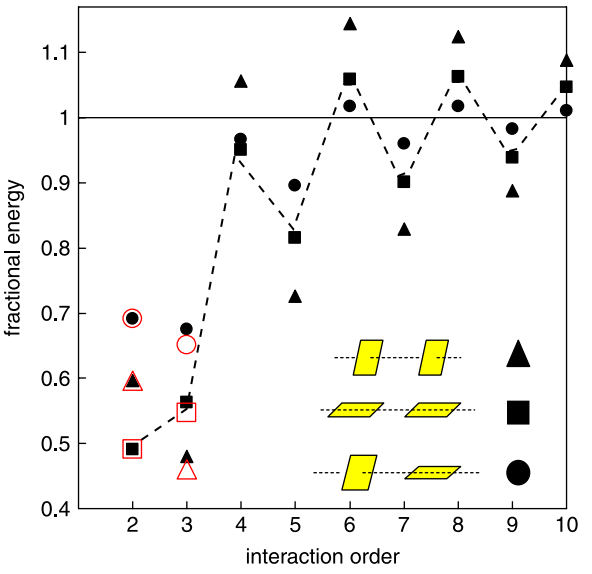

Figure 9. Fraction of total interaction energy between two square monolayers ($N = 100$), as a function of the highest order of the many-body terms included. Symbols represent various orientations. Open symbols obtained from direct calculation of two-body and three-body sums. Dotted curves are drawn to guide the eye. The triangles represent a face-to-face orientation; the squares represent an edge-to-edge orientation; the circles represent a face-to-edge orientation. Taken from [57]. © 2006; reproduced by permission of the American Institute of Physics.

>0.2, the latter falls to zero. The origin of this difference is that the interatomic function in Figure 7 is evaluated at $T = 0$, while the inter-half space function in Figure 2 is shown at room temperature. In fact, the asymptote for the interatomic problem, in general, is given by $G_{\text{inter-atomic}} = 4kT/E_{\text{atom}}$. At room temperature, this value is about 0.01.

5. Summary and future research problems

VDW interactions arise from a conceptually simple mechanism: the dynamical coupling between fluctuating dipole moments within a physical problem. Because calculations of this energy are not straightforward, simulators usually resort to convenient approximations, like pairwise summation of interaction energies. However, this approach is not accurate except for weakly polarisable media, like molecular fluids, for which the variable ν is small. See Table D1 in Appendix D for a list of materials and their polarisabilities. In the case when electronic charge is localised and $\nu < 0.23$, the CDM is well-suited to compute interactions. However, this method can be numerically cumbersome, in general. The time required to solve for eigenfrequencies for N atoms scales as N^3. In our groups we can readily examine 5000 atoms in an hour on a PC using Mathematica. In one case, the calculation has been extended to 100,000 atoms – which represents two spherical clusters of diameter 16 nm with no intervening solvent – but this required computer resources at the National Energy Research Scientific Computing Center [55].

The continuum generalisation of the CDM is appropriate for metallic systems, for which there is no constraint concerning the dielectric properties. Indeed, such a method has been employed for many simple geometries, in which cases Maxwell's equations have been solved in order to determine the normal modes of the electromagnetic field [60]. These situations include interacting half-spaces, spherical or cylindrical particles, spherical cavities and individual molecules or pairs of molecules near surfaces. However, while particle roughness and various shapes can be accounted for using the CDM with continuum electromagnetic solutions, these continuum approximations are not adequate for separations close to interatomic distances.

Many interaction models are employed in simulations, some of which are quite sophisticated in their development. The venerable LJ interaction is particularly simple in its form, partly explaining its wide use. Further, justifications of this use are that the LJ parameters (well-depth ε and hard core diameter σ) can be fit to experimental data, in many circumstances, and its asymptotic form agrees with the known r^{-6} behaviour. It is important to note, however, that this fit is usually based on data sensitive to the potential minimum, so that the resulting VDW coefficient $(C_6)_{\text{LJ}} = 4\varepsilon\sigma^6$ has no particular reason to be correct. A recent comparison of this coefficient and the 'correct' value has demonstrated this inadequacy. For various species interacting with themselves, the ratio $C_6/(C_6)_{\text{LJ}}$ has the values 0.89, 0.72, 0.85, 0.43, 0.60, 0.52, 0.49, 0.60 and 0.47 for the sequence He, Ne, H_2, O_2, Ar, N_2, CH_4, Kr and Xe, respectively [61]. Such discrepant behaviour of the LJ potential means that its long-range behaviour is in error sometimes by a factor of more than two. One plausible improvement, out of many possibilities, is to change the attractive part of the LJ interaction to this form:

$$V_{\text{attract}} = -\{f(r/\sigma)(C_6)_{\text{LJ}} + [1 - f(r/\sigma)]C_6\}/r^6. \quad (41)$$

Here, the function $f(x) = 1$ for small x and falls to zero at large x, so that the correct behaviour develops at large distance. A variety of choices are available for this 'turn-on' function.

It has been emphasised in previous sections that the Hamaker approach does not adequately describe interactions for any geometry other than those from which the Hamaker coefficient is derived. Thus, it cannot correctly predict the interaction between a single atom of Au, or a Au particle, and a Au half-space. The reason is simply that many-body interactions are critically important for metals, while the Hamaker strategy is derived explicitly

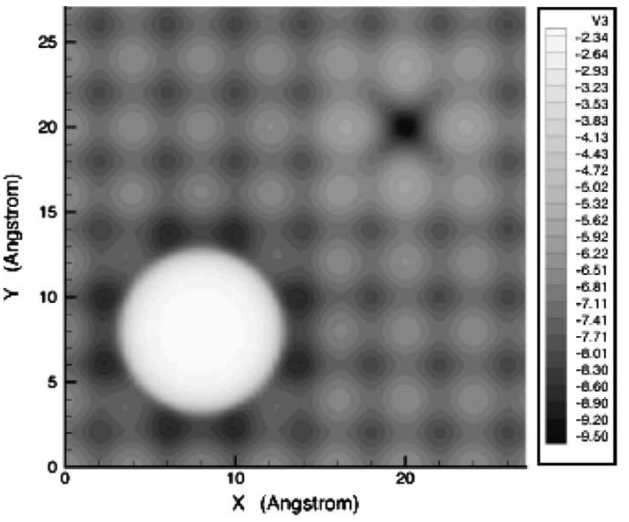

Figure 10. Potential energy experienced by an Ne atom near the surface of Mg, from which one surface atom has been moved to an overlayer position. Gray scale expresses energy shading in units of the Ne–Mg two-body well-depth, which is about 1.4 meV. Lightest contours correspond to this ratio being -2.34, while the darkest have a ratio -0.50. Taken from [63]. © 1999; reproduced by permission of the American Physical Society.

from pair interaction models. A plausible strategy worth considering in such cases is a perturbative approach, as follows. First, find simple geometrical representations of individual pieces of the system at hand, for which there exists a DLP solution. Then, supplement this zero-order result by adding the contribution attributable to the 'perturbation', i.e. the difference between the real geometry and that used in the DLP approximate calculation. An example of such approach appears in Figure 10. In that case, the potential energy in the figure was evaluated from this formula:

$$V(\mathbf{r}) = V_0(\mathbf{r}) + \Delta V(\mathbf{r}). \tag{42}$$

Here, $V_0(\mathbf{r})$ is the potential energy of an Ne atom at position $\mathbf{r}$ interacting with a perfectly flat Mg surface (computed *ab initio*, including the VDW piece [62], while $\Delta V(\mathbf{r})$ is the perturbation experienced by the Ne atom, due to both the extra Mg adatom and the missing substrate Mg atom. The two contributions to the perturbation $\Delta V(\mathbf{r})$ are necessarily approximate, but at least most of the calculated potential does not suffer from any two-body approximations.

There are several critical avenues for future study, and many researchers will be needed to answer the large variety of problems. (1) One focus of future development must be the extension of the CDM method to metallic systems or systems such as fullerenes and carbon nanotubes for which CDM fails by producing instabilities. This is not straightforward, unfortunately, because the CDM presumes a coupling of local responses to the fluctuating field. One avenue we are pursuing is to generalise the CDM to 'chunks' of matter, thus embodying the nonlocal response of the medium. While promising, we have no definitive results to report at this time for chunks of arbitrary shapes. A chunking-like approach has been used to study the cohesion of C_{60} (fullerite) by representing each C_{60} molecule as a continuous spherical shell with multipoles [64]. (2) Another avenue of research is in examining retardation in the CDM. We are examining methods similar to those that have been used for continua. (3) Larger systems are a computational challenge. Methods are required for connecting continua results for the bulk of a material system with CDM results for the interface regions where precise atomic placement could be assessed properly. In addition, it is possible that the chunking method mentioned above for metals could be used for regions of material, rather than using the CDM for individual atoms. (4) Finite temperature results require that we include effects due to the thermal energy (kT). These effects can be significant, for example in aqueous systems, since water has a permanent dipole and that permanent dipole contributes to the polarisation of the medium [65]. There are many sources of thermal fluctuations, which produce changes in material dielectric properties due to altered permanent dipoles, T-dependent positions (due to phonons), and to a small extent, electronic excitation. Nevertheless, in this review article, we have assumed $T = 0$ throughout, thus ignoring any temperature-dependent effects. (5) Applications like surface tension [21], solvophobicity/philicity, contact angles, and others can be examined at the nanoscale, even at the molecular level, using the CDM. At present, few results exist for these parameters. It is clear that for nanoscale systems, the VDW forces play a critical and often dominant role. The purpose of this review has been to show that the CDM provides a 'nanoscale Lifshitz theory' to predict the VDW energies. Many important research areas remain, providing exciting opportunities for both experienced and new researchers in this vibrant field of study.

Acknowledgements

We would like to acknowledge primary support from DOE grant DE-FG02-07ER46414, as well as numerous discussions with other scientists, including Silvina Gatica, Jerry Mahan, Jorge Sofo, Kristen Fichthorn, Leonidas Gergidis, Slava Rotkin and Adrian Parsegian. Hye-Young Kim would like to acknowledge support from the Center of Nanophase Materials Sciences, which is sponsored at Oak Ridge National Lab by DOE.

Notes

1. Email: miltoncole@aol.com
2. He2 is bound by approximately 1027 eV.

3. In one sense, the word rigorously is not correct. This expression for C3 is valid only to the first nonvanishing perturbation order in powers of the polarizability a(iv). In the Drude model of an atom interacting with a metal surface, the full result is a power series in the polarizability – that is, there are higher order terms in 1/z 6 and 1/z 9 and so on. When the metal is not perfect, such as when it responds through a dynamical image g(iw), the exact, nonretarded result can be obtained via an independent boson model (IBM) for the metal coupled harmonically to the Drude atom.

References

[1] R.E. Grisenti, W. Schöllkopf, J.P. Toennies, G.C. Hegerfeldt, T. Köhler, and M. Stoll, *Determination of the bond length and binding energy of the helium dimer by diffraction from a transmission grating*, Phys. Rev. Lett. 85 (2000), pp. 2284–2287.

[2] J.S. Rowlinson, *Cohesion: A Scientific History of Intermolecular Forces*, Cambridge University Press, Cambridge, 2002.

[3] H. Margenau and N.R. Kestner, *Theory of Intermolecular Forces*, Pergamon, Oxford, 1971. On p. 236, the label in x-axis should be R/10 not R/$\Downarrow_0$.

[4] V.A. Parsegian, *Van der Waals Forces*, Cambridge University Press, New York, 2005.

[5] I.E. Dzyaloshinskii, E.M. Lifshitz, and L.P. Pitaevskii, *The general theory of van der Waals forces*, Adv. Phys. 10 (1961), pp. 165–209.

[6] M. Schmeits and A.A. Lucas, *Physical adsorption and surface plasmons*, Prog. Surf. Sci. 14 (1983), pp. 1–52.

[7] J. Mahanty and B.W. Ninham, *Dispersion Forces*, Academic Press, New York, 1976.

[8] J.N. Israelachvili, *Intermolecular and Surface Forces*, 2nd ed., Academic, New York, 1992.

[9] H.C. Hamaker, *The London–van der Waals attraction between spherical particles*, Physica IV (1937), pp. 1058–1072.

[10] F. London, *Zur Theorie und Systematik der Molekularkrafte (On the theory and systematics of the molecular forces)*, Zeits. F. Phys. 63 (1930), pp. 245–279.

[11] R.J. Hunter, *Foundations of Colloids Science, Vol. I*, [Chapter 4, *The Theory of van der Waals Forces* by L.R. White], Clarendon Press (Oxford University Press), New York, 1986 [with corrections in 1992].

[12] S.K. Lamoreaux, *The Casimir force: background, experiments, and applications*, Rep. Prog. Phys. 68 (2005), pp. 201–236.

[13] G. Vidali, G. Ihm, H.Y. Kim, and M.W. Cole, *Potentials of physical adsorption*, Surf. Sci. Rep. 12 (1991), pp. 133–182. This article contains a compendium of information about physical adsorption, including C3 values.

[14] M. Schmeits and A.A. Lucas, *Physical adsorption and surface plasmons*, Surf. Sci. 64 (1977), pp. 176–196.

[15] J.D. Jackson, *Classical Electrodynamics*, 3rd ed., John Wiley, New York, 1999.

[16] N.W. Ashcroft and N.D. Mermin, *Solid State Physics*, Brooks/Cole, Belmont, CA, 1976.

[17] U. Fano and J.W. Cooper, *Spectral distribution of atomic oscillator strengths*, Rev. Mod. Phys. 40 (1968), pp. 441–507.

[18] J.E. Lennard-Jones, *Processes of adsorption and diffusion on solid surfaces*, Trans. Faraday Soc. 28 (1932), pp. 333–359.

[19] F. London, *Zur einige Eigenschaften und Andwendungen der Molerkulekräfte*, Zeits. F. Chem. B 11 (1930), pp. 222–251.

[20] L.W. Bruch, M.W. Cole, and E. Zaremba, *Physical Adsorption: Forces and Phenomena*, Dover, New York, 2007. See Appendix E.

[21] M.W. Cole and D. Velegol, *Van der Waals energy of a 1-dimensional lattice*, Mol. Phys. 106 (2008), pp. 1587–1596.

[22] A. Šiber, Ch. Boas, M.W. Cole, and C. Wöll, *Anomalously low probabilities for rotational excitation in HD/surface scattering: a sensitive and direct test of the potential between closed shell molecules and alkali metals*, ChemPhysChem 7 (2006), pp. 1015–1018.

[23] J. Harris and P.J. Feibelman, *Asymmetry of the van der Waals interaction between a molecule and a surface*, Surf. Sci. 115 (1982), pp. L133–L136.

[24] E. Hult, H. Rydberg, B.I. Lundqvist, and D.C. Langreth, *Unified treatment of asymptotic van der Waals forces*, Phys. Rev. B 59 (1999), pp. 4708–4713.

[25] H.B.G. Casimir and D. Polder, *The Influence of retardation on the London-van der Waals forces*, Phys. Rev. 73 (1948), pp. 360–372.

[26] D. Velegol, J.L. Anderson, and S. Garoff, *Determining the forces between polystyrene latex spheres using differential electrophoresis*, Langmuir 12 (1996), pp. 4103–4110.

[27] K.T. Tang and J.P. Toennies, *The van der Waals potentials between all the rare gas atoms from He to Rn*, J. Chem. Phys. 118 (2003), pp. 4976–4983.

[28] J.M. Standard and P.R. Certain, *Bounds to two- and three-body long-range interaction coefficients for S-state atoms*, J. Chem. Phys. 83 (1985), pp. 3002–3008.

[29] A. Kumar and W.J. Meath, *Pseudo-spectral dipole oscillator strengths and dipole-dipole and triple-dipole dispersion energy coefficients for HF, HCl, HBr, He, Ne, Ar, Kr and Xe*, Mol. Phys. 54 (1985), pp. 823–833.

[30] Z.C. Yan, J.F. Babb, A. Dalgarno, and G.W.F. Drake, *Variational calculations of dispersion coefficients for interactions among H, He, and Li atoms*, Phys. Rev. A 54 (1996), pp. 2824–2833.

[31] W.L. Bade and J.G. Kirkwood, *Drude-model calculation of dispersion forces. II. The linear lattice*, J. Chem. Phys. 27 (1957), pp. 1284–1288.

[32] F. London, *The general theory of molecular forces*, Trans. Faraday Soc. 33 (1937), pp. 8–26. In Section 6 of this paper, London dismisses the importance of multi-body interactions in dispersion forces.

[33] W.L. Bade, *Drude-model calculation of dispersion forces. I. General theory*, J. Chem. Phys. 27 (1957), pp. 1280–1284.

[34] F. Delanaye, M. Schmeits, and A.A. Lucas, *Collective effects in physical adsorption*, J. Chem. Phys. 69 (1978), pp. 5126–5132.

[35] A.A. Lucas, *Contributions Electrostatiques Collectives et Corrections Radiatives à l'Energie de Van der Waals des Cristaux Moléculaires*. Thèse de doctorat, University of Liege, 1966, unpublished.

[36] A. Lucas, *Collective contributions to the long-range dipolar interaction in rare-gas crystals*, Physica 35 (1967), pp. 353–368.

[37] D.J. Griffiths, *Introduction to Quantum Mechanics*, 2nd ed., Benjamin Cummings, New York, 2004.

[38] C. Girard and X. Bouju, *Coupled electromagnetic modes between a corrugated surface and a thin probe tip*, J. Chem. Phys. 95 (1991), pp. 2056–2064.

[39] H.-Y. Kim, J.O. Sofo, D. Velegol, M.W. Cole, and A.A. Lucas, *Van der Waals forces between nanoclusters: importance of many-body effects*, J. Chem. Phys. 124 (2006), 074504.

[40] H.-Y. Kim, J.O. Sofo, D. Velegol, M.W. Cole, and A.A. Lucas, *Van der Waals dispersion forces between dielectric nanoclusters*, Langmuir 23 (2007), pp. 1735–1740.

[41] C.F. Bohren and D.R. Huffman, *Absorption and Scattering of Light by Small Particles*, Wiley, New York, 1983.

[42] W.-H. Yang, G.C. Schatz, and R.P.J. Van Duyne, *Discrete dipole approximation for calculating extinction and Raman intensities for small particles with arbitrary shapes*, J. Chem. Phys. 103 (1995), pp. 869–875.

[43] B.M. Axilrod and E.J. Teller, *Interaction of the van der Waals type between three atoms*, J. Chem. Phys. 11 (1943), pp. 299–300.

[44] Y. Muto, *Force between non-polar molecules*, Proc. Phys. – Math. Soc. Japan 17 (1943), pp. 629–631.

[45] S.M. Gatica, M.W. Cole, and D. Velegol, *Designing van der Waals forces between nanocolloids*, Nano Letters 5 (2005), pp. 169–173.

[46] D.W. Langbein, *Theory of Van Der Waals Attraction*, Vol. 72, Springer Tracts in Modern Physics, Springer, New York, 1974.

[47] C. Kittel, *Introduction to Solid State Physics*, 8th ed., Wiley, New York, 2004.

[48] H.B.G. Casimir, *On the attraction between two perfectly conducting plates*, Proc. K. Ned. Akad. Wet. 51 (1948), pp. 793–796.

[49] Y. Imry, *Casimir zero-point radiation pressure*, Phys. Rev. Lett. 95 (2005), 080404.

[50] M.R. Aub, E.A. Power, and S. Zienau, *The influence of retardation on the London-van Der Waals force*, Philos. Mag. 2 (1957), pp. 571–572.
[51] R.R. McLone and E.A. Power, *On the interaction between two identical neutral dipole systems, one in the excited state and the other in the ground state*, Mathematika 11 (1964), p. 91.
[52] R.R. McLone and E.A. Power, *The long range van der Waals forces between non-identical systems*, Proc. R. Soc. (Lond.) A 286 (1965), pp. 573–587.
[53] W.J. Meath and J.O. Hirschfelder, *Long-range (retarded) intermolecular forces*, J. Chem. Phys. 44 (1966), pp. 3210–3215.
[54] E. Cheng and M.W. Cole, *Retardation and many body effects in multilayer film adsorption*, Phys. Rev. B 38 (1988), pp. 987–995.
[55] H.-Y. Kim and P. Kent (in preparation).
[56] M.R. Aub and S. Zienau, *Studies on the retarded interaction between neutral atoms. I. Three-body London-van der Waals interaction of neutral atoms*, Proc. R. Soc. Lond., Ser. A 257 (1960), pp. 464–476.
[57] H.-Y. Kim, J.O. Sofo, D. Velegol, and W. Cole, *Fully retarded van der Waals interaction between dielectric nanoclusters*, J. Chem. Phys. 125 (2006), 174303.
[58] E.A. Power and T. Thirunamachandran, *The non-additive dispersion energies for N molecules: a quantum electrodynamical theory*, Proc. R. Soc. Lond. Ser. A 401 (1985), pp. 267–279.
[59] H.-Y. Kim, J.O. Sofo, D. Velegol, M.W. Cole, and G. Mukhopadhyay, *Static polarizabilities of dielectric nanoclusters*, Phys. Rev. A 72 (2005), 053201.
[60] M. Schmeits and A.A. Lucas, *Physical adsorption and surface plasmons*, Prog. Surf. Sci. 14 (1983), pp. 1–51.
[61] S.M. Gatica, M.K. Kostov, and M.W. Cole, *Ordering transition of gases adsorbed on a C60 surface*, Phys. Rev. B 78 (2008), 205417.
[62] A. Chizmeshya, M.W. Cole, and E. Zaremba, *Weak binding potentials and wetting transitions*, J. Low Temp. Phys. 110 (1998), pp. 677–684.
[63] S. Curtarolo, G. Stan, M.W. Cole, M.J. Bojan, and W.A. Steele, *Computer simulations of the wetting properties of Ne on heterogeneous surfaces*, Phys. Rev. E 59 (1999), pp. 4402–4407.
[64] Ph. Lambin, A. Lucas, and J.P. Vigneron, *Polarization waves and van der Waals cohesion of C60 fullerite*, Phys. Rev. B 46 (1992), pp. 1794–1803.
[65] P. Atkins and J. de Paula, *Physical Chemistry*, 7th ed., Freeman and Company, New York, 2002. Page 693 gives some background into how permanent dipoles affect polarization.
[66] J. Mitroy and J.-Y. Zhang, *Long-range dispersion interactions. II. Alkali-metal and rare-gas atoms*, Phys. Rev. A76 (2007), 032706.
[67] J. Mitroy and J.-Y. Zhang, *Long range dispersion interactions of the low lying states of Mg with H, He, Ne, Ar, Kr and Xe*, Mol. Phys. 106 (2008), pp. 127–132.

Appendix A: classical versus quantum model of VDW interactions

Why does the classical CDM method work? To illustrate this point, consider the case of two atoms with vibrations just in the x direction, parallel to their internuclear axis. Solving this problem will lead to a simplified version and understanding of the real problem, which involves 3D vibrations. The Hamiltonian is

$$H = (p_1^2 + p_2^2)/(2m) + (k/2)(x_1^2 + x_2^2) - \lambda x_1 x_2, \tag{A1}$$

$$\lambda = e^2/(2\pi\varepsilon_0 r^3). \tag{A2}$$

This may be rewritten as a sum of a centre of mass and a relative Hamiltonian:

$$H = H_{\rm cm} + H_{\rm rel}, \tag{A3}$$

$$H_{\rm cm} = P^2/(4m) + (4/3)(k - \lambda)X^2/2, \tag{A4}$$

$$H_{\rm rel} = p_{\rm rel}^2/m + [(2k + \lambda)/3]x^2/2. \tag{A5}$$

Here, P is the centre of mass (total) momentum and $X = (x_1 + x_2)/2$ is its canonical coordinate, the centre of mass position. The difference $x = x_1 - x_2$ is the relative coordinate and $p_{\rm rel}$ is the corresponding momentum, with the reduced mass $\mu = m/2$ for that problem. Now, the original problem has been reduced to two independent, simple harmonic oscillators, with characteristic frequencies $\omega_\pm$ determined from the separate problems. A dimensionless parameter assumed to be small is the quantity proportional to λ:

$$\psi = \lambda/(2m\omega_0^2) = \alpha_0/r^3. \tag{A6}$$

The ground state energy is given by

$$E_0 = (\hbar/2)(\omega_+ + \omega_-), \tag{A7}$$

$$\omega_\pm/\omega_0 = [1 \pm 2\psi]^{1/2}. \tag{A8}$$

This result can be seen to coincide with the energy determined in our recent study of the one-dimensional chain [22], where we solved the classical problem of coupled dipole fluctuation modes. Following the math in that case, for small ψ, an expansion yields the x part of the VDW energy:

$$V_x \sim -\hbar\omega_0\psi^2/2. \tag{A9}$$

A fully 3D treatment yields the full VDW interaction, larger than V_x by a factor 3/2, viz.

$$V_{\rm total} = -C_6/r^6, \tag{A10}$$

$$C_6 = (3/4)\hbar\omega_0\alpha_0^2. \tag{A11}$$

This is London's result. This expression coincides (in the limit of identical atoms) with the following general relation for the present Drude model:

$$C_6 = [3\hbar/\pi]\int {\rm d}\omega\, \alpha({\rm i}\omega)\alpha_{\rm s}({\rm i}\omega). \tag{A12}$$

The more general result follows straightforwardly if the present procedure is adapted to that problem. The perfect agreement between the classical and quantum spectra is a general property

Table 1. Ratio of $C_{jk,\rm expt}$ to $(C_{jk})_{\rm Drude}$, computed from Equation (C2) for gases k across columns.

Gas j (E_{jj} in eV)	He	Ne	Ar	Kr	Xe	H	Li	Rb	Cs
He (26.9)	1	1.03	1.03	1.02	1.04	1.00	1.03	1.11	1.08
Na (12.8)	–	1.08	1.06	1.05	1.05	–	–	–	1.00
Mg (6.06)	1.02	1.02	1.01	1.01	1.00	1.00	1.01	1.01	1.01

The Drude model of atomic polarisability gives predictions of the attraction coefficient C usually within a few percent, and almost always within 10%. The '–' means the entry is not available. Data for $C_{\rm jk,expt}$ taken from [66,67].

Table D1. Material polarisabilities.

Material	Frequency, ω_0 ($\times 10^{16}$ rad/s)	Density, n (atom/A^3)	Polarisability, α_0 (A^3)	$n\alpha_0$
Gold	1.37	0.0590	4.048	$3/4\pi = 0.2387$
Hexane	1.65	–	–	0.0534
Sapphire	1.55	–	–	0.0975
Silica	1.74	–	–	0.0640
Silver	1.36	−0.0585	4.078	$3/4\pi = 0.2387$
Sodium	0.897	0.0253	9.417	$3/4\pi = 0.2387$
Polystyrene	1.18	–	–	0.0769

The value of $n\alpha$ is obtained from the Clausius–Mossotti equation at zero frequency, but as if only the ultraviolet contribution exists. For atomic metals (e.g. Na or Au), the value from macroscopic permittivity values are different from single atom values, due to screening. For example, atomic sodium has $\alpha_0 = 24$ A^3. Also note that for infinite system, an instability in the CDM occurs for $n\alpha_0 = 3/4\pi$, but that this value increases slightly for finite systems.

of physical problems in which the interactions are bilinear, as in Equation (A1). The CDM has this fact as its centrepiece.

Appendix B: many-body expansion of C_3

This appendix shows an explicit many-body expansion for the coefficient C_3 of the gas-surface interaction, given by Equation (5). This expansion is based on the Clausius–Mossotti relation, evaluated at a general imaginary frequency iω;, assuming that a parameter $\beta \ll 1$:

$$(\varepsilon - 1)/(\varepsilon + 2) \equiv \beta = 4\pi\alpha_s n_s/3. \quad \text{(B1)}$$

Here, α_s is the frequency-dependent polarisability of a substrate atom. Solving this relation for ε and inserting the result in the function $g(\omega)$ in Equation (5), we obtain an infinite series that converges for $\beta < 2$ (note that the convergence is well beyond the assumed value of $\beta \ll 1$):

$$g(i\omega) = [\varepsilon(i\omega) - 1]/[\varepsilon(i\omega) + 1] = (3\beta/2)\Sigma_{j=0}(-\beta/_2)^j. \quad \text{(B2)}$$

Hence, we get an explicit many-body expansion

$$C_3 = C_3^{(2)} + C_3^{(3)} + C_3^{(4)} + \cdots, \quad \text{(B3)}$$

$$C_3^{(k)} = (-1)^k[3\hbar/(4\pi)]\int d\omega\alpha(i\omega)[2\pi\alpha_s(i\omega)n_s/3]^{k-1}. \quad \text{(B4)}$$

The first term in Equation (B2) (the two-body term) appears in Equation (11). Note that successive terms in the series possess alternating signs and their ratio scales approximately as

$$C_3^{(k+1)}/C_3^{(k)} \sim -2\alpha_s n_s. \quad \text{(B5)}$$

The C_3 expansion converges if $\beta < 2$. Note that the $C_3^{(k)}$ integrals can be evaluated analytically, within the Drude approximation. For example, in the special case that the solid and the gas have the same characteristic frequency, $\omega_s = \omega_a$, we find

$$C_3^{(3)}/C_3^{(2)} = -(\pi/2)\alpha_s n_s. \quad \text{(B6)}$$

Appendix C: accuracy of the Drude model

The Drude model has long been used to characterise interactions between two atoms, between atoms and surfaces and in other situations were a simple computational model is advantageous. If it can be shown to work well in these cases, one can use the model elsewhere with some confidence. One way to assess its accuracy for computing VDW interactions is to evaluate the coefficients C_6 of the r^{-6} interactions between pairs of atoms and comparing this prediction with more reliable results for that quantity. In the following, we let C_{jk} be the value of C_6 for the case of atoms labelled

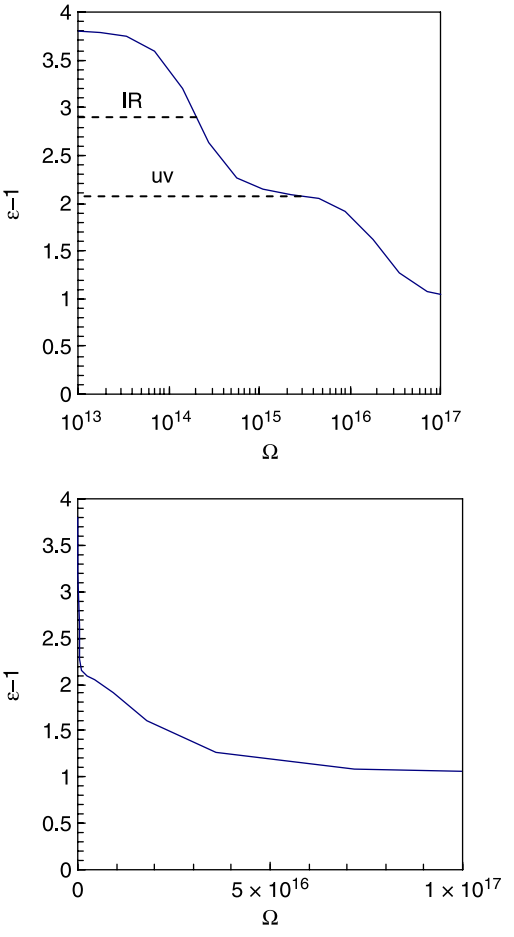

Figure D1. Permittivity function for silica. Silica is commonly represented as having two resonant peaks, one in the infrared (IR, $\omega_0 = 1.88 \times 10^{14}$ rad/s) and one in the ultraviolet (UV, $\omega_0 = 2.024 \times 10^{16}$ rad/s). Both oscillators can be represented by the Drude model for atomic oscillators. Note that, in the lower part of the figure that when plotted as a function of frequency, and not the logarithm of the frequency, the importance of the ultraviolet range is emphasised since the infrared and lower frequencies appear to be compressed. Finally, at frequencies $> 10^{17}$ rad/s, the permittivity function = 1, so that the polarisability is very nearly 0.

j and k. In making such a comparison, one needs to make a valuation of the characteristic energy E_j of each atom j. For self-consistency, we determine this energy by requiring that the self-interaction coefficient, computed with the Drude model, coincide with the state-of-the-art value, C_{jj}. Thus, E_j is determined from this 'known' quantity and the static polarisability of this atom:

$$E_j \equiv \hbar\omega_j = (4/3)C_{jj}/\alpha_j^2. \tag{C1}$$

We note in passing that use of the Drude model results in a harmonic mean *combining rule* for the corresponding energy for the mixed $(j - k)$ interaction:

$$(2/E_{jk})_{\text{Drude}} \equiv (3/2)\alpha_j\alpha_k/(C_{jk})_{\text{Drude}} = (1/E_{jj} + 1/E_{kk}). \tag{C2}$$

To test the predictions for C_{jk}, we have computed the ratio of current, best-known values of C_{jk} to those predicted $(C_{jk})_{\text{Drude}}$ with Equation (C2), for a number of systems. The results are shown in Table 1. The overall agreement is good, with a worst case 11% discrepancy corresponding to the He–Rb interaction.

It is interesting to compare the characteristic energies $\{E_j\}$ for these various species with the most common guess for that energy, the ionisation energy I_j. The ratio E_j/I_j was found to be 0.86, 1.12,1.50,1.20,1.19, 1.16, 0.35, 0.41, 0.40, 0.38 and 0.59 for the sequence H, He, Ne, Ar, Kr, Xe, H, Li, Na, Rb, Cs and Mg, respectively. Thus, the commonly used substitution of I_j for E_j is not justified, in general.

Appendix D: material polarisabilities

Throughout this review, we have used the Drude model with values for α_0 and ω_0. Typical values are shown in Table D1. It is essential for accurate calculations that these parameters be chosen judiciously. Methods for evaluating molecular parameters from bulk parameters are discussed in Ref. [40]. One method that we have commonly employed is the use of the Clausius–Mossotti equation. From this continuum equation we obtain [40]

$$\varepsilon(\mathrm{i}w) = 1 + \frac{\frac{4\pi n\alpha_0}{(1-4\pi n\alpha_0/3)}}{1 + \left(\frac{\omega}{w_0}\right)^2 \frac{1}{(1-4\pi n\alpha_0/3)}}. \tag{D1}$$

Thus, by knowing the permittivity function for a single resonant peak, values for $n\alpha_0$ and ω_0 can be calculated.

There are two important points concerning the use of Equation (D1). First, the value of $n\alpha_0$ for a particular oscillator should be the $n\alpha_0$ as if only the oscillator under consideration exists. Figure D1 shows the permittivity function for silica with two resonant peaks. The lower dashed line shows the value of the ultraviolet contribution, as if the infrared contribution did not exist. In evaluating the Drude model parameters for the ultraviolet contribution, one must use the value of $\varepsilon(0) = 2.098$ given by the lower dashed line.

Second, the resonant peak in the ultraviolet region, say in the range 1×10^{15}–1×10^{17} rad/s, is almost always the most important. Why is this range most important, at least at zero temperature where effects due to kT are not operative? The contribution to the total VDW interaction is an integral over all frequencies, as given for example by Equation (8) or (11). One finds competing factors in examining which section of the spectrum contributes most to the VDW interactions. The largest polarisability occurs at zero frequency. However, in the integration over all frequencies, the decade of frequencies from 0 to 10 rad/s has $\Delta\omega = 10$ rad/s, while the decade from 10^{15} to 10^{16} rad/s has $\Delta\omega = 9 \times 10^{15}$ rad/s. Thus, the integration occurs over a much larger range in the latter case. On the other hand, at higher frequencies – say 10^{18} rad/s where the $\Delta\omega$ are even larger, the polarisability of the material becomes vanishingly small, so that the total contribution to the integral for VDW interactions is small. Both effects are emphasised in the lower part of Figure D1.